Q. 101 – R. 65

COMMISSION INTERNATIONALE
DES GRANDES BARRAGES

VINGT SIXIÈME CONGRÈS
DES GRANDS BARRAGES
Vienne, Juillet 2018

STUDIES ON EXTENSIBILITY OF ASPHALT FACE AND EFFECTIVE REINFORCEMENT BASED ON AFRD DAMAGED BY THE EARTHQUAKE*

Tomoyuki TSUKADA
Head of Energy and Environment Division, R & D department, TEPCO RESEARCH INSTITUTE, TOKYO ELECTRIC POWER COMPANY HOLDINGS

Masaru SHIMAZAKI
Manager of Technology Department, TAISEI ROTEC CORPORATION

Takahiro MIZUNO
RESEARCH INSTITUTE, TAISEI ROTEC CORPORATION

Yousuke MATSUMOTO
Civil Engineering Department, TOKYO ELECTRIC POWER SERVICE COMPANY

JAPAN

SUMMARY

The 2011 Tohoku Earthquake triggered cracking in the asphalt face of Yashio Dam, which extended for 70–80 m from the crest almost running parallel to the abutment on both sides. This asphalt-face rock-fill dam was located about 300 km from the epicenter. The maximum observed acceleration was around 0.05 m/s^2 at the foundation and around 0.25 m/s^2 at the crest, not necessarily intense compared to the levels envisaged in the design (0.266 m/s^2 at the foundation and 1.0 m/s^2 at the crest). Nevertheless, the dam was damaged. Therefore, the conditions of cracking were studied in detail on site in combination with indoor testing and dynamic response analysis to reproduce and

** Études sur l'extensibilité du revêtement de l'asphalte et renforcement efficace basé sur l'AFRD endommagé par le tremblement de terre*

compute the behavior of the dam during the earthquake. As a result, the cracking was presumed to have appeared when strains concentrated on a block joint of the crest concrete. The further downward propagation along the slope was probably caused by strains from displacement by the earthquake and thermal contraction from the drop in the water level, which concentrated at the tips of the cracks. Indoor tests and simulations by dynamic analysis were conducted to validate the presumed causes of crack propagation. A method was devised to repair the cracks while ensuring adequate performance of the asphalt face consisting of a total of seven layers. In this method, only three layers were cut out and replaced with a material resembling a joint sealant that contained polymer-modified asphalt with great deformation following performance even in cold temperatures. The material's composition was also determined by taking the workability into account. Before the repair work, a simulation test was conducted with a sample to make sure that the method not involving cutting and replacement down to the bottom layer would provide comparable or greater deformation following performance than the existing asphalt face. The same material from the repair work was used at the crest area that experienced the strain concentration. A structure was devised and constructed to follow even a large strain after a simulation by numerical analysis.

RÉSUMÉ

Le tremblement du Tohoku de 2011 a provoqué des fissures dans le revêtement du barrage de Yashio qui s'étendaient sur 70 à 80 mètres à partir de la crête et presque parallèlement aux butées des deux côtés. Ce barrage fait d'enrochement et au revêtement en asphalte se situait à environ 300 km de l'épicentre. L'accélération maximale observée fut d'environ 0,05 m/s^2 au niveau des fondations et d'environ 0,25 m/s^2 au niveau de la crête, ce qui n'est pas forcément intense comparé aux niveaux envisagés à sa conception (0,266 m/s^2) au niveau des fondations et 1,0 m/s^2) au niveau de la crête. Néanmoins, le barrage a été endommagé. Par conséquent, les conditions de la fissuration ont été étudiées sur place en combinaison avec des tests en laboratoire ainsi qu'une analyse de réponse dynamique destinée à reproduire et à calculer le comportement du barrage pendant le tremblement de terre. Par conséquent, nous présumons que les fissures ont dû apparaître quand les déformations se sont concentrées sur la jointure d'un bloc du béton de la crête. La propagation additionnelle vers le bas le long de la pente a probablement été causée par des déformations dues au déplacement provoqué par le tremblement de terre et la contraction thermique due à la baisse du niveau de l'eau qui se sont concentrés sur les extrémités des fissures. Des tests et des simulations en laboratoire ont été menés en analyse dynamique afin de valider les causes présumées de la propagation des fissures. Une méthode a été conçue afin de réparer les fissures tout en garantissant des performances adéquates de la paroi imperméable qui est constituée en tout de sept couches. Grâce à cette méthode, seules trois couches ont été découpées et

remplacées avec un matériau qui ressemble à un mastic qui contient de l'asphalte modifié par des polymères qui présenter de grandes performances face aux déformations même à basse température. La composition du matériau a également été déterminée en prenant en compte sa maniabilité. Avant les travaux de réparation, un test de simulation a été mené avec un échantillon afin que s'assurer que la méthode qui n'implique pas la découpe et le remplacement jusqu'à la couche la plus basse pourrait fournir des performances face aux déformations comparables ou supérieures à celles de la paroi imperméable actuelle. Le même matériau des travaux de réparation a été utilisé dans la zone de la crête qui a connu une concentration de déformations. Une structure a été conçue et construite afin de faire face même à de fortes déformations d'après une simulation par analyse numérique.

Keywords: Analysis, Asphalt, Asphaltic Concrete, Behaviour, Bituminous Mastic, Combined Structure, Construction Joint, Cracking, Crest, Damage, Drawdown For Inspection, Extensibility, Flow, Impervious Asphaltic Concrete, Laboratory Test, Pervious Asphaltic Concrete, Reinforcement, Repair, Rockfill, Seismic Resistance, Strain, Temperature, Tensile Strength, Tensile Stress, Yashio Dam, Higash-Fuji Dam, Futaba Dam.

1. INTRODUCTION

The asphalt face of the Yashio Dam, an asphalt-face rock-fill dam, cracked during The 2011 off the Pacific Coast of Tohoku Earthquake (The 2011 Tohoku Earthquake). The maximum acceleration observed at the dam's bedrock during the earthquake was about 0.05 m/s^2, which is not very large compared to the 0.266 m/s^2 as envisaged in the design. Possible causes of the cracking were investigated by an in-depth on-site study of the cracks, three-dimensional dynamic analysis, laboratory test, and so on. Taking presumable causes of the cracking into account, a rational method to ensure adequate dam function was developed, applied, and implemented in the repair and reinforcement work in order to meet the power demand in the aftermath of the earthquake through swift resumption of power generation. The result of the study is presented below.

2. OVERVIEW OF YAS HIO DAM AND ITS DAMAGE FROM THE EARTHQUAKE

2.1. Overview of yashio dam

Yashio Dam is an asphalt-face rock-fill dam with a height of 90.5 m. It was constructed as a dam to contain the upstream reservoir for Shiobara Pumped

Storage Power Plant of Tokyo Electric Power Company Holdings. Fig. 1 presents the standard cross section of the dam and the structure of the asphalt face. The asphalt face consists of seven layers: the upper impermeable layer (three 50-mm-thick sublayers), the intermediate drainage layer with a thickness of 80 mm, the lower impermeable layer with a thickness of 60 mm, and the leveling and macadam layers each 40 mm thick. Any seepage water from a damaged part in the upper impermeable layer is guided safely to the inspection gallery through the intermediate drainage layer.

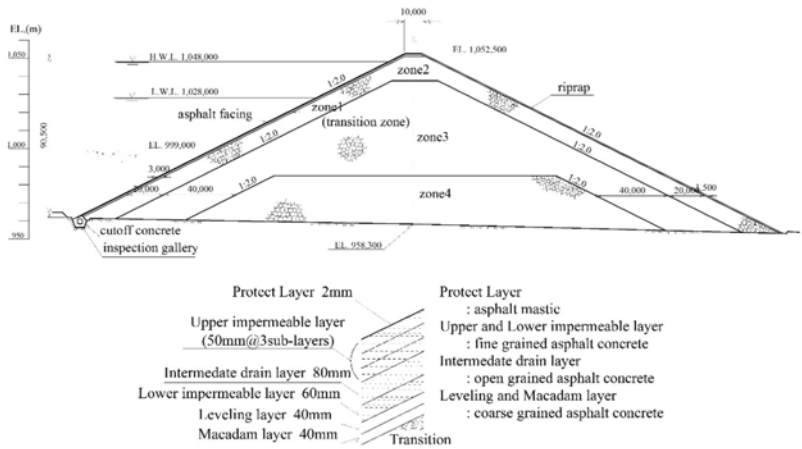

Fig. 1
Cross section of the Yashio dam
Coupe transversale du barrage de Yashio

2.2. Observation during the 2011 Tohoku earthquake

At Yashio Dam, accelerometers are installed to measure three components at a total of 13 spots in the dam's bedrock, inside and outside the dam body, and the right-bank side. Yashio Dam is about 300 km away from the epicenter of The 2011 Tohoku Earthquake. In the bedrock, the maximum acceleration was 0.053 m/s^2 along the dam axis (0.043 m/s^2 along the stream and 0.045 m/s^2 in the vertical direction). On the crest, the maximum acceleration was 0.253 m/s^2 along the steam (0.185 m/s^2 along the dam axis and 0.175 m/s^2 in the vertical direction). The maximum acceleration measured at each spot in the dam body and the measured locations are presented in Table 1 and Fig. 2.

Table 1
Maximum acceleration by The 2011 Tohoku Earthquake (unit: $x10^{-3}m/s^2$)

LOCATION	UNIT	STREAM DIRECTION	DAM AXIS DIRECTION	VERTICAL DIRECTION
Bedrock	EA-2	43	53	45
Dam crest	EA-10	174	157	105
	EA-11	253	185	175
	EA-12	252	104	156
	EA-13	66	66	43

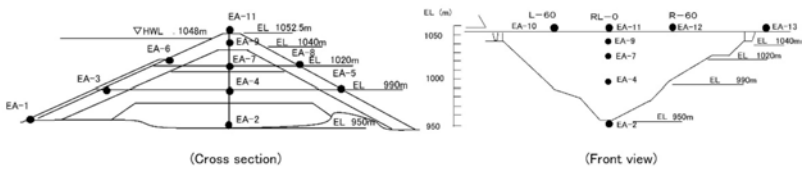

Fig. 2
Location of the seismometers
Emplacements des séismomètres

2.3. CRACKING ON ASPHALT FACE

Immediately after the earthquake, an increase was noticed in the drainage flow rate in the intermediate drainage layer, the first problem ever experienced by Yashio Dam. The ensuing inspection found a crack extending for 66.5 m in the asphalt face on the left-bank side and another 78.2-m crack on the right-bank side. Given the limitations of a visual inspection, investigation with V-shape sampling was also used at the bottom of the cracks to study them more in detail. Core samples of the cracks were obtained near the crest by using a bore with a diameter of 500 mm (Fig. 3). Thesecore samples demonstrated the extent of the cracking near the crest to the leveling and macadam layers. At the bottom tip of the crack, the cracks appeared only on the surface, on the other hand, the cracks ran deeper at the higher elevation. The study suggested that the cracks started near the crest toward the bottom of the slope. In terms of cross section, the cracking probably advanced from the surface to the deeper part.

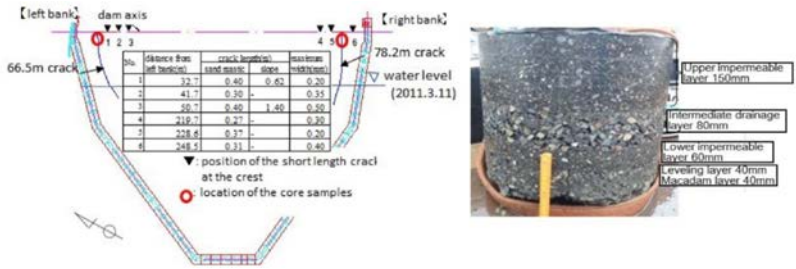

Fig. 3
Location of main and minor cracks and core sample of the asphalt face
Emplacement des fissures principales et mineures et échantillon principal du revêtement

2.4. Mixture Design and Performance of Asphalt Concrete

The composition of the fine grained asphalt concrete for the upper and lower impermeable layers of the asphalt face of Yashio Dam was determined as shown in Table 2 with the deformation following performance and slope stability kept in mind while referring to the records from existing same type dams.

Table 2
Composition of the fine grained asphalt concrete

MAX AGGREGATE SIZE (MM)	COMPOSITION (KG/TON)						
	ASPHALT	AGGREGATE		CRUSHED SAND	FINE SAND	FILLER	
		13-5 MM	5-2.5MM	2.5-0MM	2.5-0MM	STONE POWDER	ADDITIVE
13	85	166	267	276	83	115	8

The relationship between the yield strain, temperature, and strain rate in a bending test with the fine grained asphalt concrete is shown in Fig. 4. It is found that the lower the temperature is and the greater the strain rate is, the smaller the bending yield strain following performance is. Therefore, the most stringent conditions are posed in the deformation caused by an earthquake during the winter. Table 3 presents the tensile, shear, and compressive yield strains during the earthquake and the impounding process. In terms of loading speed, the water temperature during the impounding process was 5°C and the strain rate was the lowest speed of the testing machine at 0.005 mm/min. During the earthquake, the water temperature was 5°C. Air temperature was the lowest level on the site at −15°C, and the strain rate was about 10^{-2} 1/s based on the two-dimensional dynamic analysis [1].

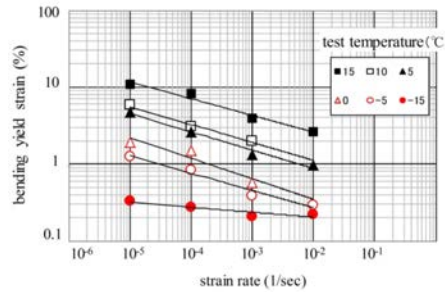

Fig. 4
Relationship between bending yield strain and strain rate
Relation entre la contrainte de déformation et le taux de déformation

Table 3
Yield strain of the fine grained asphalt concrete

TEST TEMPERATURE	ITEM	I) EARTHQUAKE		II) IMPOUNDING	
		YIELD STRAIN ($X10^{-3}$)	STRAIN RATE (1/S)	YIELD STRAIN ($X10^{-3}$)	STRAIN RATE (1/S)
5°C	Compressive	21.0	$8.0x10^{-3}$	70.0	$8.0x10^{-3}$
	Tensile	10.0	$1.0 x10^{-2}$	50.0	$1.0 x10^{-2}$
	Shear	8.8	$2.0 x10^{-2}$	130.0	$2.0 x10^{-2}$
-15°C	Compressive	12.0	$8.0 x10^{-3}$		
	Tensile	2.3	$1.0 x10^{-2}$		
	Shear	28.0	$2.0 x10^{-2}$		

Approximately 20 years after the construction, the impact of the aging of Yashio Dam was evaluated by measuring the bending yield strain with an asphalt concrete sample taken near the crest. The average strain was 2.3×10^{-3} at −5°C (average temperature when the earthquake struck) and a strain rate of 1×10^{-2} 1/s. The figure is slightly smaller than the test value of 2.9×10^{-3} (Fig. 4) used during the mixture designing. There is no pronounced deterioration on the top layer caused by ultraviolet rays given the strain of $2.1–2.5\times10^{-3}$ of the top layer, $2.0–2.5\times10^{-3}$ in the second layer, and $2.3–2.4\times10^{-3}$ in the third layer.

3. STUDY OF DAM BEHAVIOR DURING THE 2011 TOHOKU EARTHQUAKE

3.1. Analysis model

Three-dimensional dynamic analysis was conducted by equivalent linearization. The behavior of Yashio Dam, including the strain on the asphalt face, was

analyzed by reproducing the acceleration measured and recorded at the dam. With reference to Fig. 5, the analysis model included the surrounding terrain and the bedrock extending on both sides about three times the length of the dam body. In terms of depth, the model simulated the part above the accelerometer installed at the center of the bedrock (elevation of 950 m) to directly input the measurement record there. The asphalt face was not simulated in the model as it was assumed to behave in an integrated manner with the dam body.

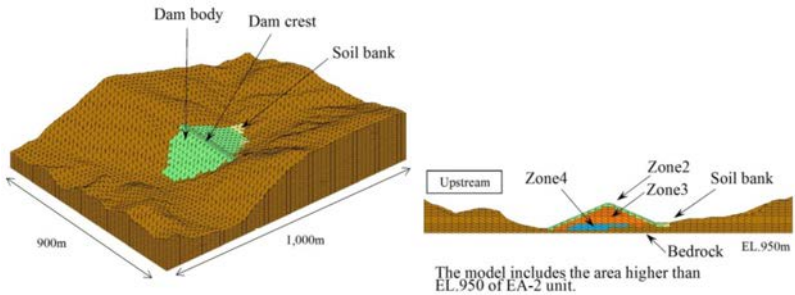

Fig. 5
Three dimensional numerical analysis model
Modèle d'analyse numérique tridimensionnelle

3.2. Physical properties used for analysis

Properties of the bedrock were assigned based on test values from the past. Nonlinearity of the dam materials was assigned according to past test results using the Hardin-Drnevich (H-D) model and Sawada's rate distribution based on actual measurements from existing dams. The shear rigidity based on the past test results was employed after making sure that the transfer function obtained from the observation records from microearthquakes in the past was consistent with the dominant frequency. The analysis resulted in an excessively large acceleration compared to the acceleration observed during The 2011 Tohoku Earthquake. Accordingly, the damping property was adjusted to hmax = 30% whereas the test value of hmax = 20% [2].

3.3. Analysis results

The earthquake response analysis targeted the 80 seconds before to 80 seconds after the main quake. Over the time history of acceleration in each part of

the crest, the figure based on analysis was slightly bigger than the measurement. But their consistency was deemed satisfactory. The distribution of the maximum acceleration in each spot over the entire duration is shown on the left side of Fig. 6. The right side of Fig.6 presents the distribution of the maximum strain on the surface elements of the dam body. The elements on the upstream surface experienced the largest tensile, compressive, and shear strains in a spot about 1/5 of the way below the center of the crest. All these strains were much smaller than the yield strain. The tensile strain was about 1/10 the yield strain, whereas the compressive strain was about 1/60 and the shear strain was about 1/100. The evaluation with the three-dimensional FEM analysis model could not identify a strain exceeding the yield strain or consistency between the crack location and the location of the maximum strain. Further study was conducted in detail to estimate the cracking mechanism.

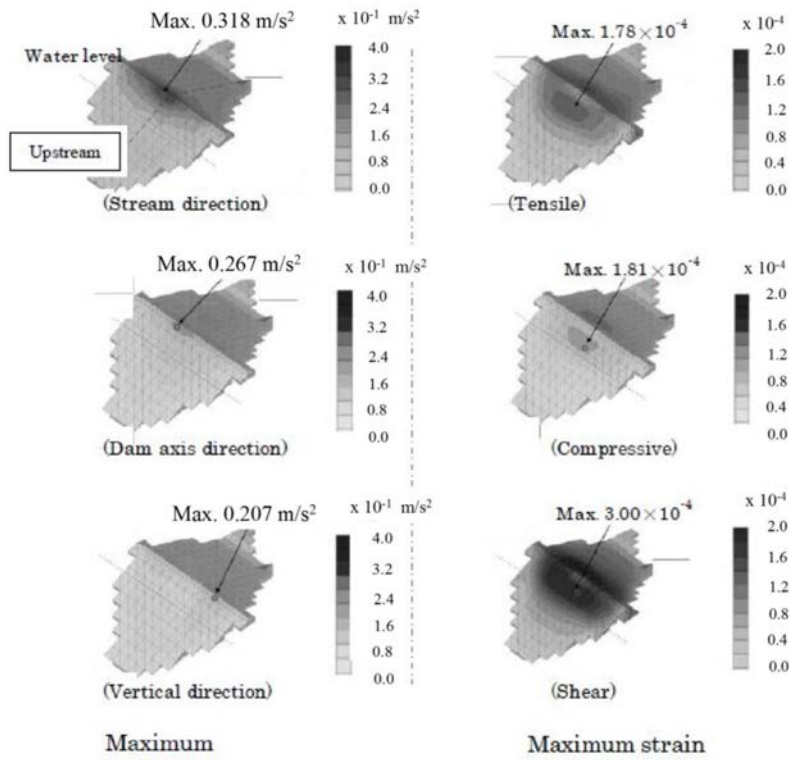

Fig. 6
Maxium acceleration and strain at the surface by the analysis
Accélération maximale et contrainte à la surface par l'analyse

4. ESTIMATING THE CRACKING MECHANISM

With reference to Fig. 7, in the structure around the crest of Yashio Dam, the space between the concrete block and asphalt face is filled with sand mastic. Sand mastic has about 10 times greater deformation following performance than fine grained asphalt concrete. Aside from a crack extending for about 70–80 m on each side of the asphalt face, three shorter cracks with lengths between 0.3 and 1.8 m were identified on each side of the part near the crest (Fig. 3). Each of thesecracks ran from block joints of the crest concrete through the sand mastic filling to the asphalt face. The finding suggested the possibility of the cracking being triggered by concentrated strain as a result of the opening of joints of concrete blocks.

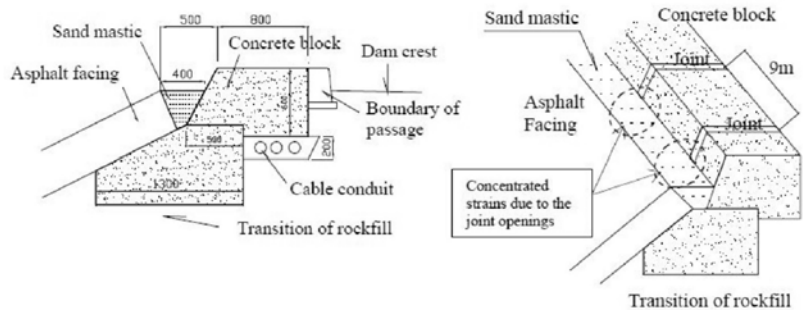

Fig. 7
Asphalt face structure at the dam crest
Structure du revêtement à la crête du barrage

The cracking mechanism was studied on the basis of the results of the abovementioned three-dimensional dynamic analysis. The time history of the displacement of crest elements was extracted from the results of the analysis to check the time history of the strain by concentrating different displacements in each joint of the concrete blocks. The resulting strain exceeded the tensile yield strain of the sand mastic in each joint. The exceeded timing was much earlier near the positions of cracking on both sides. Later, greater strains appeared toward the center of the dam body away from thesecracks (Fig.8). No major cracking appeared in the central area; this was probably due to the released stress as a result of earlier cracking.

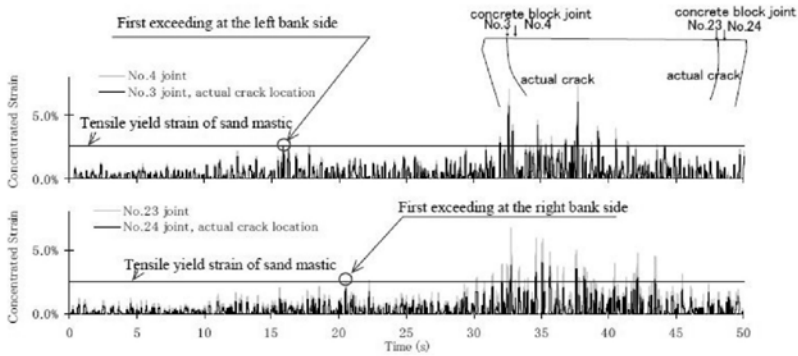

Fig. 8
Concentrated strain by estimates at the actual crack location
Contrainte concentrée par estimation à l'endroit réel de la fissure

5. VALIDATION OF THE CRACKING MECHANISM

The cracking mechanism as estimated above was validated with the cracks until they advanced for 70–80 m along the abutment.

5.1. Evaluation of crack propagation by testing the cutout beam of the asphalt concrete

A possible cause of the crack propagation from the crest to the bottom of the crack (despite not very large displacements associated with the earthquake) was the concentration of strains at the tip of each crack. Accordingly, a method for tracking the toughness of concrete after the appearance of cracking was applied to the fine grained asphalt concrete so as to evaluate the yield tensile strength (strain) at the tip of a crack after the cracking took place. A sample was taken from the exposure test yard constructed next to the dam site. The exposure test yard is located about 200 m from the right-bank side. The material and timing of paving was the same as the dam body. The altitude of the crest and the direction of the slope are the same as those of the dam. The sample was 60 mm wide, 56 mm tall, and 250 mm long with the span length of 168 mm (Fig. 9).

The test was conducted at an air temperature of −5°C (average temperature on the day the earthquake struck), a water temperature of 5°C, and loading rate

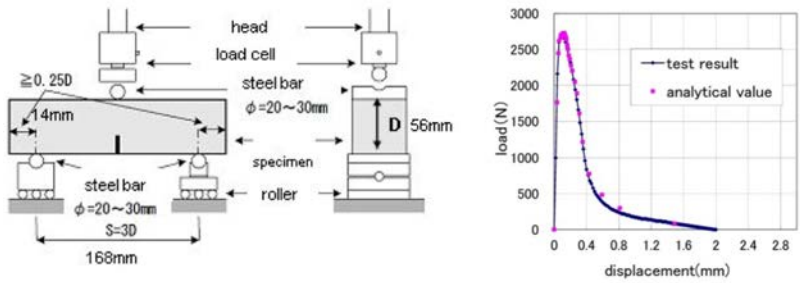

Fig. 9
Equipment of bendig test by beam with cutout and reproduction result of relation between displacement and load
Équipement des tests de déformation par faisceau avec découpe et reproduction résultant de la relation entre le déplacement et la charge

of 50.4 mm/min (the same as the strain rate of 1×10^{-2}/s in the bending test with a sample without a cutout). The tension softening curve was estimated based on the relationship between the load and displacement from the test results. An example of the reproduced test results is shown on the right side of Fig. 10. The estimated tension softening curve at a temperature of −5°C is shown on the left side of Fig. 10 and the curve at a temperature of 5°C is shown on the right side. According to the approximation of these tension softening curves using two lines, the bonding stress becomes 0 with a crack width of 1.15 mm at a temperature of −5°C and 1.65 mm at a temperature of 5°C.

Based on the results of this test and the aforementioned three-dimensional dynamic analysis, the displacement at the tip of the cracking was assumed to

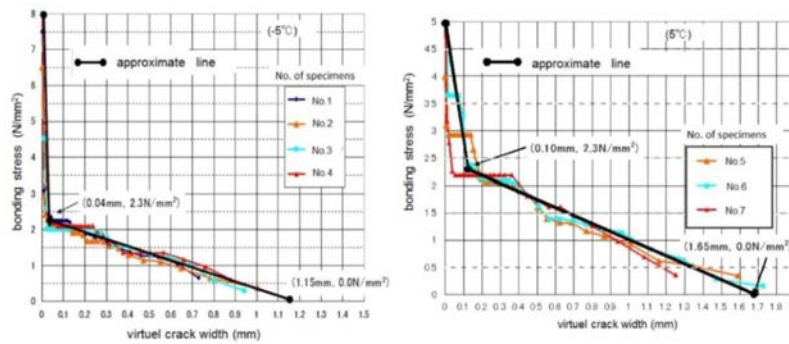

Fig. 10
Relation between virtuel crack width and bonding stress
Relation entre la largeur des fissures virtuelles et les contraintes d'adhérence

equal the width of a crack once it appears in the asphalt face near the crest. Thus, the crack propagation was predicted by tracing the timing of displacement at nodal points of the asphalt face according to the following procedure.

(1) Calculate the yield strain corresponding to the width of the crack based on the relationship between the crack width and bonding stress in Fig. 10 (yield strain according to the crack width = Bonding stress ÷ Elastic modulus).

(2) Calculate the change in the distance between neighboring nodal points near the cracking according to time by three-dimensional FEM analysis. Divide the change with the initial distance between the nodal points to obtain the average strain between nodal points.

(3) If the change in the distance between the nodal points next to the concrete joint of the crest that experienced cracking is treated as the crack width, crack propagation is assumed when the corresponding yield strain falls short of the average strain between nodal points as obtained in (2).

The initial value of the yield strain is 2.3×10^{-3} (temperature of −5°C and strain rate of 1×10^{-2}1/s) according to the result of the bending test with the core sample obtained near the crest.

(4) Repeat Step (3) until the direction of crack propagation is finally determined.

The result of prediction according to the abovementioned procedure is presented in Fig. 11. On both sides of the dam, the predicted crack propagation resembled the actual cracking caused by the earthquake. The finding led to the conclusion that the widening of cracks from the earthquake triggered the crack propagation to the area near the water surface.

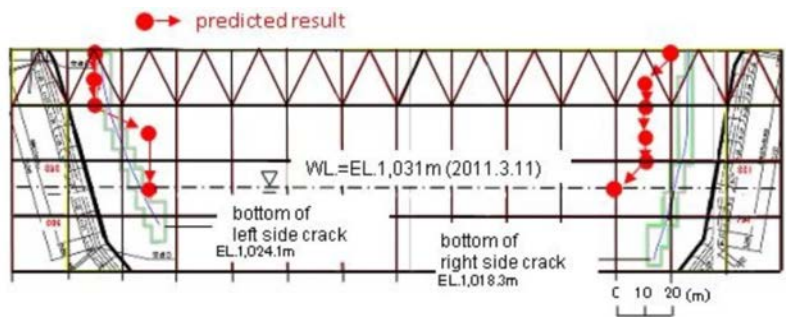

Fig. 11
Crack propagation prediction result
Résultat de la prédiction de la propagation des fissures

5.2. Evaluation of Temperature Stress

The three-dimensional dynamic analysis and the tension softening curve of the fine grained asphalt concrete suggested the possibility of crack propagation to the area near the water surface. Actually, Fig. 11 shows that the cracking reached 7–13 m below the water surface during the earthquake. Another possible cause of the crack propagation was the contraction of the asphalt face due to the drop in temperature associated with the changes in the level of impounded water and the outside air temperature after the earthquake, as well as the temperature of the impounded water, and the flow rate in the intermediate drainage layer. Accordingly, the temperature stress was also evaluated. Fig. 12 presents measurements of the outside air temperature, impounded water temperature (0.5 m below the surface), and flow rate of intermediate drainage from immediately before the earthquake until March 21.

Immediately after the earthquake, on both March 12 and 13, impounded water at Yashio Dam was pumped up and the water level of the dam was changed from an elevation of around 1,030 to 1,034 m before the water level dropped to generate power. The intermediate drainage flow rate increased corresponding to the rise in the water level. But, the increase is larger during the rise of the water level on March 13. A possible reason is the growth of the crack in length or width due to the drop in the temperature by about 10°C as the water level dropped from March 12 to March 13 and the part under the water with a temperature around 5°C was exposed to air with a temperature around −5°C. The total amount of intermediate drainage flow rate can be automatically measured on both sides of the dam. Furthermore, from March 14 to March 17, the temperature dropped by about 20°C in the area initially above the water and 15°C in the area initially under the water. The resulting contraction may have caused crack propagation and widening. Therefore, in order to determine whether the crack propagation after the aforementioned crack propagation caused by the earthquake was caused by the temperature stress, the results of the temperature stress test for the fine grained asphalt concrete used for the asphalt face of Yashio Dam were evaluated in combination with the calculation of the temperature stress associated with the external restraint stress in accordance with the cracking condition.

There are test results from measurement of temperature stress generated by dropping the temperature of fine grained asphalt concrete by 10°C from the initial level at a rate of 2°C per hour. In this test, a sample with a size of 25 mm × 25 mm × 260 mm was fixed on both ends in a cold tank with a temperature controlled with a tolerance of ±0.1°C before it was cooled down from a certain temperature at a certain cooling rate until it broke. The load was recorded every five minutes.

The rupture strength due to temperature stress is about 3 N/mm^2 at about −30°C. Fig. 13 translates into a strain of around 8×10^{-4} by assigning the linear expansion coefficient of 20 μ/°C for fine grained asphalt concrete. Given a constant linear expansion coefficient, the relationship between the temperature and elastic

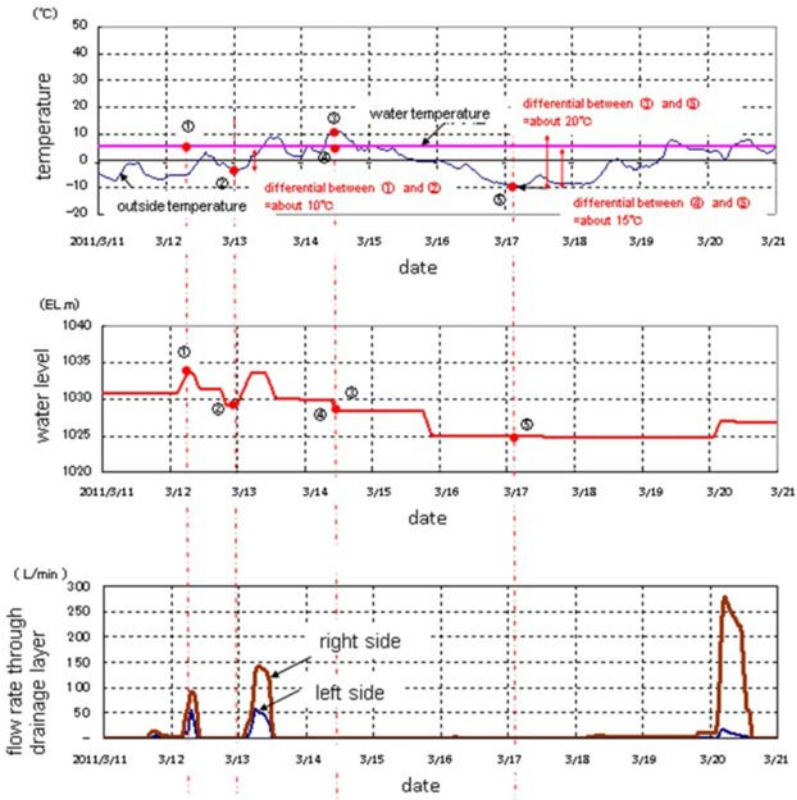

Fig. 12
Outside temperature / water temperature, water level and flow rate through the intermediate drainage layer
Température extérieure/température de l'eau, niveau d'eau et débit à travers la couche de drainage intermédiaire

modulus can be calculated based on the relationship between the temperature and temperature stress. The ambient temperature dropped down to −10°C after the earthquake on March 11, which may have generated a certain amount of temperature stress. The temperature stress from external restraint of the asphalt face is generated when the transition rockfill restrains the contraction of the asphalt face in response to the temperature decrease.

We found that the restricted range of foundation of asphalt face was limited and it was about 20 ~ 30 m around the cracks (Fig. 14). We confirmed it by estimating relationship between measured change of the crack width, outer

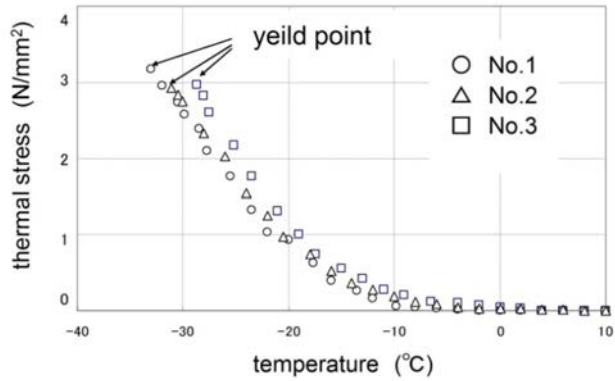

Fig. 13
Result of thermal stress test
Résultat du test de contrainte thermique

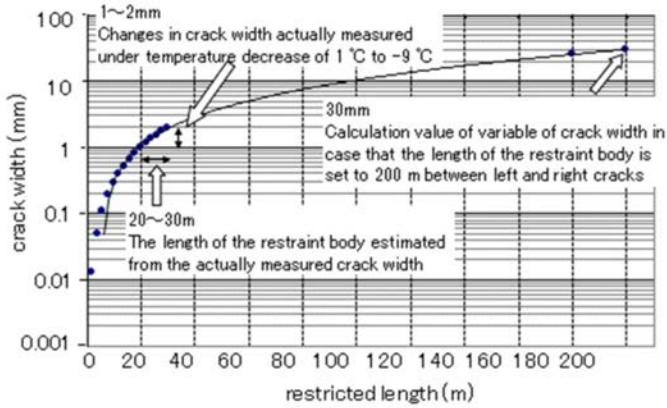

Fig. 14
Relationship between the restricted length (0-220m) and the crack width
Relation entre la longueur restreinte et la largeur de la fissure

temperature and temperature stress calculated by the elastic modulus of the asphalt face corresponding to temperature and foundation of asphalt face (rock-fill), based on the results of the temperature stress test of asphalt concrete and existing research [3].

If the restricted length is between 20 and 30 m, a temperature decrease of 15°C is expected to widen a crack by 1.8–3.5 mm (Fig. 15). Such an increase

would quite possibly result in a strength of 0 and further crack propagation when the crack width reaches 1.15 mm at a temperature of −5°C and 1.65 mm at a temperature of 5°C according to Fig. 10.

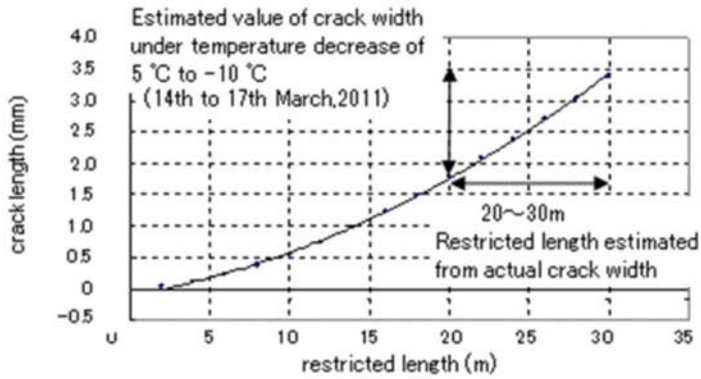

Fig. 15
Relationship between the restricted length (0-30m) and the crack width
Relation entre la longueur restreinte et la largeur de la fissure

6. CONSIDERATION OF A METHOD FOR REPAIRING CRACKS

6.1. Selection of Repair Materials and Methods

In the past, the asphalt face of Higashi-Fuji Dam (an asphalt face earth dam) [4] damaged by an earthquake was repaired by making fine grained asphalt concrete with Super Flexphalt (SF) [5], a polymer modified asphalt developed as a repair material to provide expandability even in cold temperatures. Although the complete replacement of cracked parts with the same material was considered, Yashio Dam had to address the power shortage in the immediate aftermath of the earthquake. Quick recovery was an urgent priority, which included resuming operation of the Shiobara Pumped Storage Power Plant, to prepare for increased power demand during the summer. An enormous amount of work would have been required for more than four months to completely cut and remove the cracked parts down to the bottom layer. The most effective way to expedite the repair work was to minimize the range of cutting and removal of parts around the cracks.

A solution was sought by leaving cracks beneath a certain layer while minimizing the negative impact with a newly devised structure. Accordingly, with reference to Fig. 16, a repair method was devised that involved cutting and removing the top two impermeable layers around the cracking, and fill in SF-based

asphalt mastic (SF mastic) after cutting each crack on the third layer in a strip with a width of around 10 cm. In order to address the risk of reflection cracking toward the upper layers, an asphalt-impregnated non-woven sheet used in the emergency recovery was laid both to suppress the slope movement (flow) after putting SF mastic in place and to serve as a cover during pavement of the top layer. An anti-fluidization agent was applied to the asphalt mastic filling to account for the fluidization during the construction and infiltration into the intermediate drainage layer underneath. A plant fiber material [6] with proven effectiveness in suppressing slope fluidization under high temperatures was selected and mixed in the agent with a weight ratio of 3% according to a laboratory test (Table 4).

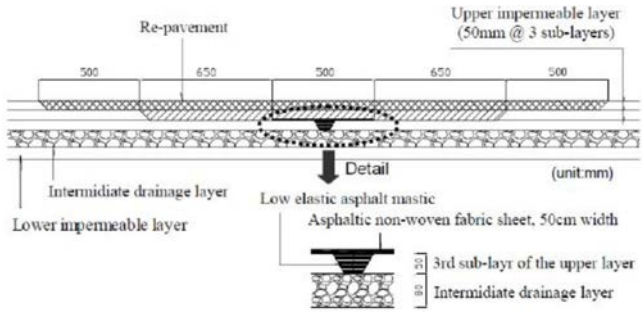

Fig. 16
Cross section of repairing work for upper impermeable layer
Coupe transversale des travaux de réparation pour la couche imperméable supérieure

Table 4
Composition of the SF mastic

Composition (%)		
Super Flexphalt	Filler	Plant fiber
40	57	3

6.2. Mechanical characteristics of the repair work

A sample was prepared by simulating the cross section of a repaired segment to check the performance in an experiment. A bending test was carried out with a sample simulating the cross section of repaired asphalt face while assuming that the cracking left in the intermediate drainage layer and thereunder would form an opening. The sample simulated the cross section of the asphalt face, consisting of the top two impermeable layers, the third layer with a 10-cm wide strip filled with SF mastic in the middle, and the intermediate drainage layer. A load was applied at the center of the top edge in order to open a slit made in the intermediate drainage layer to simulate a crack. For comparison, the same

test was conducted with a sample simulating the cross section of the top two impermeable layers, the third layer, and the intermediate drainage layer without a slit. Fig. 17 presents the resulting load-displacement curves. The repaired asphalt face did not break until the amount of the deflection reached three times that of the deflection that resulted in the failure of a sample simulating the existing cross section. Although the interface between the fine grained asphalt concrete on the top and SF mastic broke under further load, the joint between the SF mastic and fine grained asphalt concrete maintained closecontact.

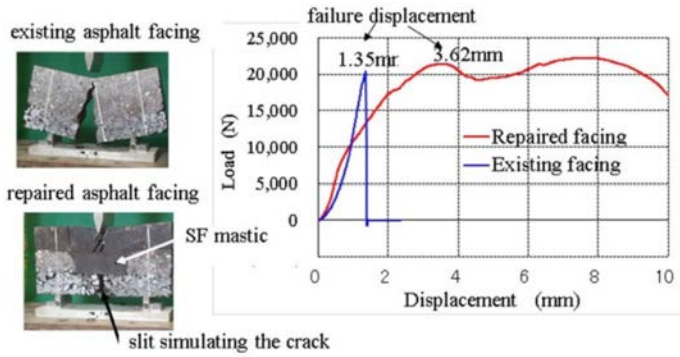

Fig. 17
Result of the bending tests of repairing structure
Résultat des essais de déformation de la structure en cours de réparation

7. REINFORCEMENT WORK

A structure was explored that would prevent cracking in the asphalt face even when strains concentrated on a block joint of the crest concrete. According to the three-dimensional dynamic analysis, a concrete joint of the crest opened by about 1 mm during The 2011 Tohoku Earthquake. But, the reinforcement was designed to follow a joint displacement of about 50 mm by anticipating a major earthquake. The reasons are the subsidence of the crest by a few dozen centimeters as experienced by Ishibuchi Dam and other CFRDs after major earthquakes, as well as the tightened body of Yashio Dam thanks to the thorough construction work. In order to follow a displacement of a few centimeters caused by a major earthquake, a crack with a width of 50–100 mm was filled with the material to repair it. In terms of workability, a width of up to 100 mm was deemed appropriate to avoid unwanted flow during the construction work. With the repair width of 100 mm, admissible displacement was confirmed to be about 50 mm (the strain without a rupture in the bending test with SF mastic was 0.5 (strain during the stress peak was 0.4 at a temperature of −15°C and strain rate of 1×10^{-2} s^{-1})). The structure of the reinforcement work was explored by conducting two-dimensional FEM elastic analysis along the dam axis while simulating an opening of 50 mm in

a block joint of the crest concrete. In the structure before the reinforcement, strains experienced in each part of the asphalt face were examined by simulating forced displacement of a crest concrete joint underneath the asphalt face near the crest. As a result, large tensile strains were experienced over an extensive area. Strains concentrated on the strip of SF mastic filled in the joint with a width of 100 mm, which reduced strains on the surrounding area. But, the strain near the interface with SF mastic exceeded the fracture strain of the existing fine grained asphalt concrete. Thus, the part surrounding SF mastic was replaced with fine grained asphalt concrete with the mixture that used SF with a high deformation following performance. The fracture strain of the SF-based fine grained asphalt concrete is 6.6×10^{-3} at −15°C and the strain rate of 1×10^{-2} s^{-1}, which is about three times greater than that of the existing fine grained asphalt concrete as shown in Table 3. Ultimately, with reference to Fig. 18, SF mastic was placed with a width of 100 mm on top of the joint and a strip of 200 to 530 mm on each side was replaced by SF-based fine grained asphalt concrete. As a result, none of the generated strains exceeded the fracture strain of the materials, and up to 5.3×10^{-3} of the tensile strain in the SF mastic could be followed. The reinforcement structure near the crest concrete of Yashio Dam based on the analysis is presented in Fig. 19. This method is believed to be effective for the construction of the same type of dams or modification of the same type of existing dams with structures that likewise lead to concentrated strains.

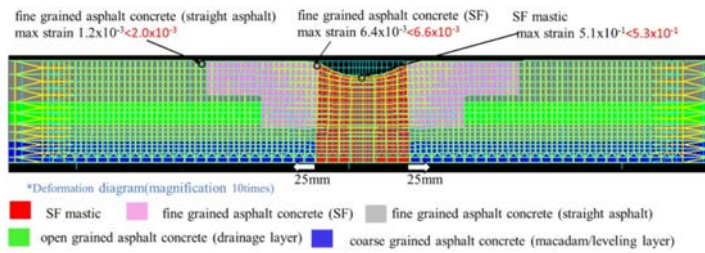

Fig. 18
Result of the FEM analysis for design of reinforcement structure
Résultat de l'analyse FEM pour la conception de la structure de renforcement

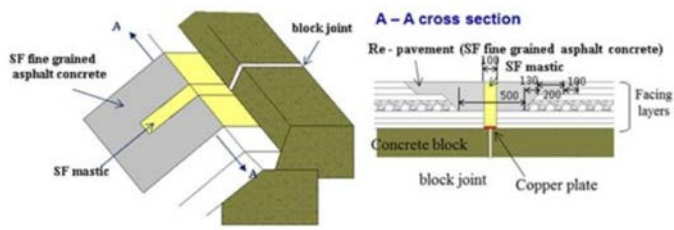

Fig. 19
Outline of the reinforcement structure at dam crest
Aperçu de la structure de renforcement de la crête du barrage

8. CONCLUSION

During The 2011 Tohoku Earthquake on March 11, Yashio Dam registered a maximum acceleration of about 0.05 m/s^2 in the foundation and a maximum acceleration of about 0.25 m/s^2 in the crest. Cracking appeared in the asphalt face even though the observed acceleration was smaller than the acceleration envisaged in the design of this asphalt-face rock-fill dam. Cracking is presumed to have appeared due to the concentration of the strain on a block joint of the crest concrete. The concentration of the strain at the tips of the cracking turned out to be a possible reason for its downward propagation even to the area with relatively small displacement. Further crack advancement to the area below the level of impounded water at the moment the earthquake struck was possibly because of the widening of cracks from the temperature strain associated with exposure to cold temperatures when the water level dropped. For these reasons, once cracks appear in asphalt face, it may propagate even with small strains generated later. Any spots where localized strains may be concentrated probably need special consideration in terms of a structure and material that can mitigate such strains. Moreover, cracking may propagate further during the winter from damage on a dam asphalt face when it is exposed to cold temperatures when the water level drops. The water level needs to be lowered in a careful manner for any studies or other purposes to ensure stable performance while adequately checking the behavior of the amount of water leakage. During the operation of the same type of dam, any damage on the asphalt face must be addressed while paying proper attention to its properties.

The repair and reinforcement work was carried out with an eye to its swift completion, good endurance, and prevention of cracking recurrence during a strong earthquake. Quick response was possible because visual inspection of the damage and repair from the surface were possible—advantages offered by this type of dam. As for the structure around the block joint of the crest concrete presumed to be the cause of cracking of the asphalt face associated with the earthquake, a material with a good deformation following performance was adopted along with the edge trimming design, which can follow up to 50% of a strain.

ACKNOWLEDGEMENTS

We would express our sincere thanks to Tatsuo Ohmachi, Professor Emeritus, Tokyo Institute of Technology and Advisor to Japan Dam Engineering Center (JDEC), Dr. Norihisa Matsumoto, Advisor to JDEC, Mr. Joji Yanagawa, President, JDEC and Mr. Mitsuaki Mizuno, former director of Japan Water Agency for their kind guidance.

REFERENCES

[1] ISHII K, KAMIJO M. Design for asphaltic concrete facing of Sabigawa upper dam. ICOLD congress, San Fransisco, Q61-R.19, 1988.

[2] TSUKADA T., YAMAMOTO H., SHIMADA Y., UCHITA Y. & TAKASAWA K. Study on behavior of AFRD during earthquake and the conducted reinforcement. ICOLD annual meeting, Seattle, 2013.

[3] YOSHIOKA Y.,YONEZAWA T. Study on intensity of external restraint for temperature stress analysis of mass concrete, JCI annual meeting, 1986 (in Japanese)

[4] NAKAMURA Y., OHNE Y., OKUMURA T., NOMURA K., SHIMAZAKI M. & MIZUNO T. Earthquake damages and remedial works for earth dam with asphalt facing. ICO LD annual meeting, St. Petersburg, 2007.

[5] SHMAZAKI M., TSUNOO T.& KASAHARA A. Application of low temperature properties improvement asphalt to repair work of rock fill dam with asphalt facing, Journal of Japan Society of Civil Engineers, Division E, vol. 67, 2011 (in Japanese)

[6] KAINUMA N., SHINOHARA T. & ITOH T. An experimental study on slope stabilizing additives for impermeable membrane mixture of fill-type dam. ASCE, No.516/V-27, 1995.(in Japanese)